A Novel Glycolysis-Related Gene Signature that can Predict the Prognosis of Glioblastoma Patients

Chaocai Zhang
Hainan Medical University
Minjie Wang
Huazhong University of Science and Technology Tongji Medical College
Fenghu Ji
Huazhong University of Science and Technology
Yizhong Peng
Huazhong University of Science and Technology Tongji Medical College
Jiannong Zhao (hngh_neurosurgery@163.com)
https://orcid.org/0000-0001-7367-0652
Jiandong Wu
Suzhou Municipal Hospital

Primary research

Keywords: Glioblastoma, glycolysis-related gene, prognostic prediction

Posted Date: June 22nd, 2020

DOI: https://doi.org/10.21203/rs.3.rs-36552/v1

Abstract

Background: Glioblastoma (GBM) is one of the most common primary intracranial malignancies, with limited treatment options and poor overall survival (OS). Metabolic changes in GBM have attracted wide attention in recent years, and one of the main metabolic features of cancer cells is the high level of glycolysis. Therefore, it is necessary to identify novel biomarkers associated with glycolysis in GBM.

Methods: In this study, we performed gene set enrichment analysis and profiled four glycolysis-related gene sets, which revealed 327 genes associated with biological processes. Univariate and multivariate Cox regression analyses were performed to identify genes for constructing a risk signature, and we identified ten mRNAs (B4GALT7, CHST12, G6PC2, GALE, IL13RA1, LDHB, SPAG4, STC1, TGFBI and TPBG) in the Cox proportional hazards regression model for GBM.

Results: Based on this gene signature, we divided patients into high-risk (with poor outcomes) and low-risk (with better outcomes) subgroups. Multivariate Cox regression analysis showed that the prognostic power of this ten-gene signature is independent of clinical variables. Furthermore, we validated this model in two other GBM databases (Chinese Glioma Genome Atlas (CGGA) and REMBRANDT). In the functional analysis, the risk signature was associated with almost every step of cancer progression, such as adhesion, proliferation, angiogenesis, drug resistance and even an immune-suppressed microenvironment.

Conclusion: The 10 glycolysis-related gene risk signature could serve as an independent prognostic factor for GBM patients and might be valuable for the clinical management of GBM patients.

Background

Glioblastoma (GBM), with an annual incidence of 3.22 per 100,000, remains the most common and aggressive primary adult brain tumour [1, 2]. Common therapeutic regimens include maximal safety surgical resection, followed by radiotherapy and chemotherapy. Moreover, targeted therapy, immunotherapy and tumour treating fields (TTFs) are also widely used in the treatment of GBM [3, 4]. Despite applying the best standard of care, patients diagnosed with GBM usually face a dismal prognosis, with a survival time of less than 2 years for most patients [5]. In recent years, many studies have shown that altered metabolism in cancer cells is pivotal for cancer growth and progression [6–8]. Aerobic glycolysis (Warburg effect), one of the hallmarks of cancer, states that cancer cells produce lactate from the absorbed glucose as a substrate for mitochondrial oxidative phosphorylation, even under normoxic conditions [9]. This in turn enables cancer cells to successfully compete with normal cells for glucose uptake to maintain uninterrupted growth [10]. In GBM, glycolysis has been suggested to correlate with tumour proliferation, invasion, angiogenesis, and chemotherapy/radiotherapy resistance [11–14]. In addition, glycolysis could shape the tumour microenvironment (TME) and regulate immune and inflammatory responses [15]. Thus, a deeper understanding of glycolysis could be an important step towards the individualized treatment of GBM.

In this study, we aimed to discover novel glycolysis-related prognostic markers in GBM patients using gene set enrichment analysis (GSEA) and Cox multivariate regression models to analyse whole genome expression profile data sets. We profiled the hallmark gene sets in 167 GBM patients with whole mRNA expression data from The Cancer Genome Atlas (TCGA) database. We identified 327 mRNAs significantly associated with glycolysis and established a ten-gene risk signature that can effectively predict patient outcomes. Notably, the glycolysis-related risk signature could independently identify patients in the high-risk group with poor prognosis. In addition, functional analysis demonstrated that the risk signature was associated with almost every step of cancer progression, such as adhesion, proliferation, angiogenesis, drug resistance and even an immune-suppressed microenvironment.

Methods

Clinical information of the patients and genome expression data

The transcriptional profile and clinical data of patients with low-grade glioma (LGG) and GBM were extracted from the TCGA database (https://cancergenome.nih.gov/). Clinical information, including the total number of patients (n = 696, including 529 LGG patients and 167 GBM patients), gender, age, Karnofsky Performance Status (KPS) score, radiotherapy, chemotherapy, IDH status and MGMT promoter methylation status, was collected for the study. Validation information from the Repository for Molecular Brain Neoplasia Data (REMBRANDT, microarray) and Chinese Glioma Genome Atlas (CGGA, microarray) data sets were downloaded from GlioVis (http://gliovis.bioinfo.cnio.es/).

GSEA

GSEA (http://www.broadinstitute.org/gsea/index.jsp) was used to explore whether the identified sets of genes demonstrated significant differences between the two groups [16]. The expression levels of all mRNAs in LGG and GBM were analysed using GSEA_4.0.3. Normalized *p*-values ($p < 0.05$) and normalized enrichment scores (NESs) were used to determine functions to be investigated in further analysis. Gene set variation analysis (GSVA) was used to explore biological processes and Kyoto Encyclopedia of Genes and Genomes (KEGG) pathways associated with the risk signature [17]. Ten associated gene sets with differences between the high-risk group and the low-risk group in the TCGA data set (GBM HGU133A) were selected using the R package “limma”, and an adjusted *p*-value < 0.05 was considered statistically significant.

Prognostic analysis

The associations between the expression level of each mRNA and patient overall survival (OS) were calculated using a univariate Cox model. In the univariate Cox analysis, mRNAs with *p*-values less than 0.05 were considered statistically significant. Afterward, multivariable Cox analysis was used to evaluate

the weight of mRNAs as independent predictors of survival. These analyses were conducted using the R package “survival”.

Statistical analysis

The candidate genes were classified into risk (hazard ratio (HR) > 1) and protective (0 < HR < 1) types. Based on the multivariate Cox regression analysis results, a prognostic risk score formula was established using a linear combination of the expression levels weighted with the regression coefficients. The risk score formula is described as follows:

Risk score = expression of gene 1 × β1 + expression of gene 2 × β2 +.....+ expression of gene n × βn. We classified 167 patients with GBM into high-risk and low-risk subgroups using the median risk score as the cutoff. Kaplan-Meier (KM) curves and the log-rank test were used to validate the prognostic significance of the risk score in stratified analysis. Student's t test was used to examine the differential expression of the optimal genes in LGG and GBM tissues. All of the statistical analyses were performed using SPSS 19.0 and R 3.6.3 software. We also researched the genetic alterations of the prognosis-related genes in GBM through cBioPortal (http://www.cbioportal.org/). The chi-square test was used to assess the relationships between the risk score and clinical parameters, and the Bonferroni method was used to perform pairwise comparisons within multi-group comparisons [18].

Results

Glycolysis-related gene sets differ significantly between LGG and GBM samples

The mRNA expression and clinical data of all patients were obtained from TCGA. We found all glycolysis-related gene sets in the Molecular Signatures Database (MSigDB) version 7.1 to represent well-defined glycolysis states or processes. GSEA was performed to explore whether the identified sets of genes showed significant differences between the LGG and GBM samples. Ultimately, we found that four gene sets, including GO_GLYCOLYTIC_PROCESS, HALLMARK_GLYCOLYSIS, KEGG_GLYCOLYSIS_GLUCONEOGENESIS, and REACTOME_GLYCOLYSIS, were significantly enriched with normalized *p*-values < 0.05 (Table 1, Fig. 1). We then selected the four gene sets, which contained 327 specific genes, for further analysis.

Table 1
Significantly enriched glycolysis-associated gene sets.

Optimal Gene Sets	SIZE	NES	NOM p-val	FDR q-val
GO_GLYCOLYTIC_PROCESS	105	1.509	0.043*	0.043*
HALLMARK_GLYCOLYSIS	200	2.031	< 0.001***	< 0.001***
KEGG_GLYCOLYSIS_GLUCONEOGENESIS	62	1.703	0.014*	0.014*
REACTOME_GLYCOLYSIS	72	1.763	0.012*	0.012*

Identification of glycolysis-related genes associated with survival in patients with progressive GBM

To identify novel genetic biomarkers associated with the outcomes of patients with GBM, univariate Cox proportional hazards regression was applied to 327 genes that were enriched via glycolysis. A total of 27 genes were significantly correlated with OS ($p < 0.05$) and were entered into a stepwise multivariate Cox regression analysis. Finally, ten independent genes (B4GALT7, CHST12, G6PC2, GALE, IL13RA1, LDHB, SPAG4, STC1, TGFBI and TPBG) (Table 2) were selected via multivariable Cox regression analysis in R according to the Akaike information criterion [19]. Finally, a gene-based prognostic model was established to evaluate the survival risk of each patient as follows: Risk score = expression of B4GALT7 × 2.0604 + expression of CHST12 × 1.4322 + expression of G6PC2 × (-2.8374) + expression of GALE × 1.4081 + expression of IL13RA1 × 1.0801 + expression of LDHB × (-3.2119) + expression of SPAG4 × 0.3957 + expression of STC1 × 0.4413 + expression of TGFBI × (-1.4198) + expression of TPBG × 0.5223. Then, the differential expression of the ten genes in LGG and GBM samples was also investigated. Eight genes (B4GALT7, CHST12, GALE, IL13RA1, SPAG4, STC1, TGFBI and TPBG) were significantly upregulated in GBM samples, and two genes (G6PC2 and LDHB) were significantly upregulated in LGG samples ($p < 0.0001$, Fig. 2).

Table 2
Detailed information on the ten prognostic mRNAs significantly associated with overall survival in patients with GBM.

mRNA	Ensemble ID	Location	β (Cox)	HR (95% CI)	*p*-value
B4GALT7	ENSG00000027847	Chr5: 177,600,102–177,610,330	2.0604	7.8488 (0.8616–71.5017)	0.0676
CHST12	ENSG00000136213	Chr7: 2,403,489-2,448,484	1.4322	4.1879 (1.1431–15.3426)	0.0306*
G6PC2	ENSG00000152254	Chr2: 168,901,223 – 168,910,000	-2.8374	0.0586 (0.0069–0.4932)	0.0091**
GALE	ENSG00000117308	Chr1: 23,795,599 – 23,800,754	1.4081	4.0882 (0.9346–17.8829)	0.0615
IL13RA1	ENSG00000131724	ChrX: 118,726,954 – 118,794,533	1.0801	2.9449 (1.1305–7.6718)	0.0270*
LDHB	ENSG00000111716	Chr12: 21,635,342 – 21,657,971	-3.2119	0.0403 (0.0020–0.7950)	0.0348*
SPAG4	ENSG00000061656	Chr20: 35,615,829 – 35,621,094	0.3957	1.4853 (0.9105–2.4232)	0.1131
STC1	ENSG00000159167	Chr8: 23,841,929 – 23,854,806	0.4413	1.5547 (0.9410–2.5686)	0.0849
TGFBI	ENSG00000120708	Chr5: 136,028,988 – 136,063,818	-1.4198	0.2418 (0.1027–0.5689)	0.0011**
TPBG	ENSG00000146242	Chr6: 82,362,983 – 82,367,420	0.5223	1.6858 (1.1448–2.4826)	0.0082**

Association between the risk score and patient outcomes

Using the ten-mRNA signature, we calculated the risk scores for each patient with GBM and ranked them in order of increasing risk scores (Fig. 3a). Figure 3b shows the risk score, OS (in years) and life status of 167 patients in the GBM data set, ranked in order of increasing risk scores. Patients with high risk scores had higher mortality rates than patients with low risk scores. Then, the 167 patients in the entire GBM data set were classified into the high-risk group (n = 83) and the low-risk group (n = 84) using the median risk score as the threshold. The KM analysis showed a significant difference in the outcomes of patients

in the high-risk group and the low-risk group (log-rank test $p < 0.001$; Fig. 3c). Patients in the high-risk group had significantly worse survival than those in the low-risk group. To evaluate how well the ten-mRNA signature can predict prognosis, receiver operating characteristic (ROC) curve analysis was carried out. The area under the curve (AUC) for the ten-mRNA signature was 0.771, 0.847 and 0.713 for one-year, three-year and five-year survival, respectively (Fig. 3d), demonstrating the reliable prognostic performance of the ten-mRNA signature for predicting survival in the entire dataset. To confirm that the gene signature performs better than the single gene biomarkers, we performed KM and ROC curve analyses, and the results supported our hypothesis. When the ten genes were each taken as a single biomarker, their prognostic performance was not better than that of the ten-mRNA signature (Fig. 3e).

The risk score generated from the ten-mRNA signature as an independent prognostic indicator

To compare the risk score and conventional clinical factors, we performed univariate and multivariate Cox proportional hazards analyses, which included risk score, gender, age, KPS score, radiotherapy, chemotherapy, IDH status and MGMT promoter methylation status as covariables, to evaluate the importance of these indicators in the patient cohort. We found that risk score (HR: 2.357; 95% confidence interval [CI]: 1.734–3.204; $p < 0.001$), age (HR: 2.576; 95% CI: 1.515–4.379; $p < 0.001$), radiotherapy (HR: 0.298; 95% CI: 0.160–0.555; $p < 0.001$), chemotherapy (HR: 0.488; 95% CI: 0.267–0.892; $p = 0.020$), IDH status (HR: 0.229; 95% CI: 0.056–0.943; $p = 0.041$), and MGMT promoter methylation status (HR: 0.539; 95% CI: 0.316–0.920; $p = 0.023$) were associated with patient survival in the univariate analysis. In addition, risk score, age and radiotherapy had remarkable independent prognostic value not only in the univariate analysis but also in the multivariate analysis ($p < 0.05$), which indicates that the prognostic value of the ten-gene signature is significant for survival prediction. These results indicated that the risk score was robust in predicting the prognosis of patients with GBM (Table 3).

Table 3
Univariate and multivariate analyses of each clinical feature.

Clinical feature	Univariate analysis			Multivariate analysis		
	HR	95% CI of HR	*p*-value	HR	95% CI of HR	*p*-value
Risk score (Low-risk/High-risk)	2.357	1.734–3.204	< 0.001***	1.822	1.252–2.651	0.002**
Gender (Female/Male)	1.332	0.788–2.250	0.284	1.167	0.592–2.299	0.655
Age (< 65/≥65)	2.576	1.515–4.379	< 0.001***	2.270	1.274–4.044	0.005**
KPS (< 60/≥60)	0.983	0.964–1.002	0.082	0.984	0.960–1.009	0.215
Radiotherapy (Untreated/Treated)	0.298	0.160–0.555	< 0.001***	0.348	0.131–0.926	0.035*
Chemotherapy (Untreated/Treated)	0.488	0.267–0.892	0.020**	1.468	0.559–3.855	0.436
IDH status (Wild-type/Mutant)	0.229	0.056–0.943	0.041*	0.583	0.122–2.793	0.499
MGMT promoter status (Unmethylated/Methylated)	0.539	0.316–0.920	0.023*	0.879	0.457–1.689	0.698

Validation of the risk signature

A total of 237 GBM samples in the CGGA data set and 181 GBM samples in the REMBRANDT data set were collected and used as two validation data sets to assess the performance of the risk signature. The K-M survival curves showed that patients with higher risk scores had poorer prognosis than those with lower risk scores (Fig. 4a, CGGA, $p < 0.05$; and 4b, REMBRANDT, $p < 0.05$). The AUCs of the ROC curves for predicting the 1-, 3- and 5-year survival of GBM patients in the CGGA data set were 0.589, 0.603 and 0.618, respectively (Fig. 4c), and those in the REMBRANDT data set were 0.561, 0.614 and 0.593 (Fig. 4d). These results indicated that the risk signature performed well for predicting the survival of GBM patients.

Associations between the risk signature and clinical characteristics

To explore the associations between the risk signature and clinical characteristics, we first constructed a heatmap to present the distribution trends of gender, age, KPS score, transcriptome subtype, IDH1 status and MGMT promoter methylation status between the low-risk and high-risk groups in the TCGA database. As shown in Fig. 5, the high-risk group tended to contain more patients older than 65 years, whereas samples with IDH1 mutations were all included in the low-risk group, and samples with different

transcriptome subtypes seemed to have distinct distributions in the two risk groups. Meanwhile, there were no significant differences between the low-risk and high-risk groups in gender, KPS score, and MGMT promoter status. To be more intuitive, the chi-square test was used to verify the proportion differences of each factor (age, gender, molecular subtypes, MGMT promoter methylation status and IDH1 status) between the low-risk and high-risk groups (Table 4). The results demonstrated that patients older than 65 years had more high-risk proportions, patients with wild-type IDH1 GBM had more high-risk proportions and patients with GBM of the mesenchymal subtype had the highest high-risk proportions (Bonferroni method).

Table 4
Associations between the signature risk score and clinical features.

Clinical feature	Risk score		χ^2	*p*
	High risk n (%)	Low risk n (%)		
Gender			0.011	0.917
Female	29(49.15%)	30(50.85%)		
Male	54(50.00%)	54(50.00%)		
Age			3.974	0.046*
< 65	47(43.93%)	60(56.07%)		
>=65	36(60.00%)	24(40.00%)		
KPS score	Fisher's Exact Test			0.572
< 60	3(42.86%)	4(57.14%)		
>=60	55(47.01%)	62(52.99%)		
Transcriptome subtype		Fisher's Exact Test		< 0.0001****
Classical	20(38.46%)	32(61.54%)		
Mesenchymal	54(73.97%)	19(26.03%)		
Neural	4(57.14%)	3(42.86%)		
Pro-neural	1(5.26%)	18(94.74%)		
IDH1 status			7.669	0.006**
Wild type	78(52.35%)	71(47.65%)		
Mutant	1(9.09%)	10(90.91%)		
MGMT promoter status			1.271	0.260
Unmethylated	37(50.00%)	37(50.00%)		
Methylated	22(40.00%)	33(60.00%)		

Functional analysis of the risk signature

GSVA was used to explore the biological processes and KEGG pathways associated with the risk signature. As shown in Fig. 6a, several biological processes relevant to necrosis, leukocyte migration involved in the inflammatory response, positive regulation of macrophage chemotaxis and regulatory T cell differentiation were enriched in the high-risk group. Regarding KEGG pathways, the high-risk group was positively correlated with apoptosis, focal adhesion, the MAPK and JAK-STAT signalling pathway,

the VEGF signalling pathway, ABC transporters and so on (Fig. 6b). In brief, these results revealed that the risk signature was correlated with almost every step of cancer progression.

Discussion

In recent years, cancer research on energy metabolism has attracted attention. Moreover, a large number of researchers have supported tumour metabolism as a critical determinant of glioma progression. In addition to TME-related factors, oncogenic mutations also modulate glioma metabolism to promote tumour cell proliferation and evasion of drug therapy [20, 21]. It has been demonstrated that the cancer genotype and the TME shape the metabolic reprogramming of GBM and are thus potential therapeutic targets. Moreover, regulators of GBM metabolism can be useful tools for prognostication, diagnosis and therapy [20]. The Warburg effect is a phenomenon in which metabolism shifts to aerobic glycolysis rather than mitochondrial oxidative phosphorylation, which is a typical biochemical adaptation in GBM. Targeting glycolysis-related regulatory genes is an ideal therapeutic strategy for GBM. Several glycolysis regulatory genes have been reported, including hexokinase 2 (HK2) and PTEN-induced kinase 1 (PINK1), where the inhibition of HK2 and activation of PINK1 in preclinical GBM models have shown therapeutic benefit [22, 23].

However, due to the high heterogeneity of GBM, targeting a single gene is often unable to effectively control tumour progression; moreover, single gene expression is easily interfered with by many external factors, and it is difficult for these biomarkers to independently and accurately predict the survival rate of patients. Therefore, in the present study, we constructed a statistical model containing multiple glycolysis-related genes and combined the function of each gene to improve the prediction efficiency. This kind of model has been confirmed in many other solid tumours and is superior to a single biomarker in predicting tumour prognosis [24–26].

Ten glycolysis-related biomarker genes (B4GALT7, CHST12, G6PC2, GALE, IL13RA1, LDHB, SPAG4, STC1, TGFBI and TPBG) were found to be statistically and biologically significant in the discrimination of LGGs from GBM in the present study, and six genes (CHST12, G6PC2, IL13RA1, LDHB, TGFBI and TPBG) were demonstrated to be significantly correlated with the prognosis of GBM patients (Table 2). Among these biomarker genes, LDHB is a dehydrogenase and a critical switch that regulates glycolysis and OXPHOS. It has been demonstrated that the expression of LDHB alone was not able to predict a difference in OS, but the concomitant expression of LDHB and CCNB1 was able to identify medulloblastoma patients with a significantly worse prognosis [27]. Transforming growth factor-beta-induced (TGFBI) is an exocrine protein that has been found to be able to promote the development of glioma, nasopharyngeal carcinoma, bladder cancer and other tumours [28, 29]. In a recent study, Guo Sk and colleagues showed that TGFBI was upregulated in glioma cells and played a promoting role in the growth and motility of U87 and U251 cells. Their results suggested that TGFBI has the potential to be a diagnostic marker and to serve as a target for the treatment of gliomas [30]. IL-13 receptor subunits α1 and α2 of the IL-13R complex are overexpressed in GBM. Jing Han and his colleagues showed that high IL13Rα1 with or without IL13Rα2 expression was associated with poor prognosis in patients with high-grade gliomas, but

there was no correlation between IL-13Rα1 mRNA and IL-13Rα2 mRNA expression. Their findings have important implications in understanding the role of IL-13R in the pathogenesis of GBM and potentially other cancers [31]. Although these genes can independently predict tumour prognosis to some extent, our results demonstrated that the ten-mRNA signature has better prognostic significance than the corresponding single biomarkers. Moreover, by using KM and ROC curve analyses of GBM, we verified our statistical results in the CGGA and REMBRANDT data sets and confirmed that the risk signature performed well in predicting the survival of GBM patients (Fig. 4). Therefore, this glycolysis-related gene signature can predict tumour prognosis more accurately and guide treatment more comprehensively.

We also constructed a heatmap to present the associations between the risk signature and clinical characteristics in the TCGA database. Our results indicated that elderly age, the mesenchymal subtype and wild-type IDH1 were significantly correlated with higher risk scores (Table 4) (Fig. 5). Consistent with mainstream views, elderly patients, the mesenchymal subtype and wild-type IDH1 usually predict an unfavourable prognosis [32, 33]. Moreover, by using GSVA to explore the biological processes and KEGG pathways associated with the risk signature, we noticed that the risk signature was correlated with almost every step of oncogenesis and tumour progression, including adverse biological processes and signal transduction pathways (Fig. 6). Currently, many studies have elucidated the aggressive behaviours associated with GBM glycolysis and attempted to find ways to target GBM glycolysis, such as through Myc, PGK1, SIRT3 and HK1 [34–37]. Therefore, our results once again confirm the reliability of the risk score in predicting the prognosis of GBM and provide new potential targets for targeting glycolysis.

Conclusion

In conclusion, we identified and validated a risk signature with 10 glycolysis-related genes associated with the survival of patients with GBM, where higher risk scores indicate unfavourable outcomes. Moreover, these glycolysis-related genes could be potential prognostic targets in GBM therapies. Our findings may provide novel insights for GBM research and guidance for individual therapy.

Abbreviations

GBM: Glioblastoma; OS: Overall Survival; CGGA: Chinese Glioma Genome Atlas; TTFs: Tumour Treating Fields; TME: Tumour Microenvironment; GSEA: Gene Set Enrichment Analysis; TCGA: The Cancer Genome Atlas; LGG: Low-Grade Glioma; KPS: Karnofsky Performance Status; REMBRANDT: Repository for Molecular Brain Neoplasia Data; NESs: Normalized Enrichment Scores; KEGG: Kyoto Encyclopedia of Genes and Genomes; KM: Kaplan-Meier; MSigDB: Molecular Signatures Database; HK2: hexokinase 2; PINK1: PTEN-induced kinase 1

Declarations

Ethics approval and consent to participate

Not applicable.

Consent for publication

Not applicable.

Availability of data and materials

The datasets used and/or analyzed in the present study are available from the corresponding author on reasonable request.

Competing interests

The authors declare that they have no competing interests.

Funding

Supported by the Hainan Provincial Natural Science Foundation of China (Funding code: 819QN351), Key research and development projects of Hainan Province (Funding code: ZDYF2019173)

Authors' contributions

MW and CZ conceived, designed, analyzed the data, and write the manuscript. CZ and YP helped to search for some relevant papers for this research. MW and FJ analyzed the data and generated the figures and tables. Jiannong Zhao and Jiandong Wu guided the research process. All authors read and approved the final manuscript.

Acknowledgements

We would like to thank everyone who take part in this study.

References

1. Ostrom QT, Cioffi G, Gittleman H, Patil N, Waite K, Kruchko C, et al. CBTRUS statistical report: primary brain and other central nervous system tumors diagnosed in the United States in 2012-2016. Neuro Oncol. 2019;21:v1-100.
2. Stupp R, Taillibert S, Kanner A, Read W, Steinberg D, Lhermitte B, et al. Effect of tumor-treating fields plus maintenance temozolomide vs maintenance temozolomide alone on survival in patients with

glioblastoma: a randomized clinical trial. JAMA. 2017;318:2306-16.

3. Cloughesy TF, Mochizuki AY, Orpilla JR, Hugo W, Lee AH, Davidson TB, et al. Neoadjuvant anti-PD-1 immunotherapy promotes a survival benefit with intratumoral and systemic immune responses in recurrent glioblastoma. Nat Med. 2019;25:477-86.
4. Molinaro AM, Taylor JW, Wiencke JK, Wrensch MR. Genetic and molecular epidemiology of adult diffuse glioma. Nat Rev Neurol. 2019;15:405-17.
5. Ostrom QT, Bauchet L, Davis FG, Deltour I, Fisher JL, Langer CE, et al. The epidemiology of glioma in adults: a "state of the science" review. Neuro Oncol. 2014;16:896-913.
6. Fakhri S, Moradi SZ, Farzaei MH, Bishayee A. Modulation of dysregulated cancer metabolism by plant secondary metabolites: a mechanistic review. Semin Cancer Biol. 2020. doi: 10.1016/j.semcancer.2020.02.007.
7. Martinez-Outschoorn UE, Peiris-Pages M, Pestell RG, Sotgia F, Lisanti MP. Cancer metabolism: a therapeutic perspective. Nat Rev Clin Oncol. 2017;14:11-31.
8. Gentric G, Mieulet V, Mechta-Grigoriou F. Heterogeneity in cancer metabolism: new concepts in an old field. Antioxid Redox Signal. 2017;26:462-85.
9. Ganapathy-Kanniappan S, Geschwind JF. Tumor glycolysis as a target for cancer therapy: progress and prospects. Mol Cancer. 2013;12:152.
10. Ganapathy-Kanniappan S. Molecular intricacies of aerobic glycolysis in cancer: current insights into the classic metabolic phenotype. Crit Rev Biochem Mol Biol. 2018;53:667-82.
11. Fu Y, Wang D, Wang H, Cai M, Li C, Zhang X, et al. TSPO deficiency induces mitochondrial dysfunction, leading to hypoxia, angiogenesis, and a growth-promoting metabolic shift toward glycolysis in glioblastoma. Neuro Oncol. 2020;22:240-52.
12. Kathagen-Buhmann A, Schulte A, Weller J, Holz M, Herold-Mende C, Glass R, et al. Glycolysis and the pentose phosphate pathway are differentially associated with the dichotomous regulation of glioblastoma cell migration versus proliferation. Neuro Oncol. 2016;18:1219-29.
13. Lan F, Qin Q, Yu H, Yue X. Effect of glycolysis inhibition by miR-448 on glioma radiosensitivity. J Neurosurg. 2019:1-9. doi: 10.3171/2018.12.jns181798.
14. Son B, Lee S, Kim H, Kang H, Jeon J, Jo S, et al. Decreased FBP1 expression rewires metabolic processes affecting aggressiveness of glioblastoma. Oncogene. 2020;39:36-49.
15. Kesarwani P, Kant S, Prabhu A, Chinnaiyan P. The interplay between metabolic remodeling and immune regulation in glioblastoma. Neuro Oncol. 2017;19:1308-15.
16. Powers RK, Goodspeed A, Pielke-Lombardo H, Tan AC, Costello JC. GSEA-InContext: identifying novel and common patterns in expression experiments. Bioinformatics. 2018;34:i555-64.
17. Hanzelmann S, Castelo R, Guinney J. GSVA: gene set variation analysis for microarray and RNA-seq data. BMC Bioinformatics. 2013;14:7.
18. Curtin F, Schulz P. Multiple correlations and Bonferroni's correction. Biol Psychiatry. 1998;44:775-7.

19. Vrieze SI. Model selection and psychological theory: a discussion of the differences between the Akaike information criterion (AIC) and the Bayesian information criterion (BIC). Psychol Methods. 2012;17:228-43.
20. Bi J, Chowdhry S, Wu S, Zhang W, Masui K, Mischel PS. Altered cellular metabolism in gliomas - an emerging landscape of actionable co-dependency targets. Nat Rev Cancer. 2020;20:57-70.
21. Venneti S, Thompson CB. Metabolic reprogramming in brain tumors. Annu Rev Pathol. 2017;12:515-45.
22. Agnihotri S, Golbourn B, Huang X, Remke M, Younger S, Cairns RA, et al. PINK1 is a negative regulator of growth and the warburg effect in glioblastoma. Cancer Res. 2016;76:4708-19.
23. Agnihotri S, Mansouri S, Burrell K, Li M, Mamatjan Y, Liu J, et al. Ketoconazole and posaconazole selectively target HK2-expressing glioblastoma cells. Clin Cancer Res. 2019;25:844-55.
24. Niyazi M, Pitea A, Mittelbronn M, Steinbach J, Sticht C, Zehentmayr F, et al. A 4-miRNA signature predicts the therapeutic outcome of glioblastoma. Oncotarget. 2016;7:45764-75.
25. Cheng W, Ren X, Cai J, Zhang C, Li M, Wang K, et al. A five-miRNA signature with prognostic and predictive value for MGMT promoter-methylated glioblastoma patients. Oncotarget. 2015;6:29285-95.
26. Jiang L, Zhao L, Bi J, Guan Q, Qi A, Wei Q, et al. Glycolysis gene expression profilings screen for prognostic risk signature of hepatocellular carcinoma. Aging (Albany NY). 2019;11:10861-82.
27. de Haas T, Hasselt N, Troost D, Caron H, Popovic M, Zadravec-Zaletel L, et al. Molecular risk stratification of medulloblastoma patients based on immunohistochemical analysis of MYC, LDHB, and CCNB1 expression. Clin Cancer Res. 2008;14:4154-60.
28. Zou J, Huang R, Li H, Wang B, Chen Y, Chen S, et al. Secreted TGF-beta-induced protein promotes aggressive progression in bladder cancer cells. Cancer Manag Res. 2019;11:6995-7006.
29. Atkins RJ, Stylli SS, Kurganovs N, Mangiola S, Nowell CJ, Ware TM, et al. Cell quiescence correlates with enhanced glioblastoma cell invasion and cytotoxic resistance. Exp Cell Res. 2019;374:353-64.
30. Guo SK, Shen MF, Yao HW, Liu YS. Enhanced expression of TGFBI promotes the proliferation and migration of glioma cells. Cell Physiol Biochem. 2018;49:1097-109.
31. Han J, Puri RK. Analysis of the cancer genome atlas (TCGA) database identifies an inverse relationship between interleukin-13 receptor alpha1 and alpha2 gene expression and poor prognosis and drug resistance in subjects with glioblastoma multiforme. J Neurooncol. 2018;136:463-74.
32. Lapointe S, Perry A, Butowski NA. Primary brain tumours in adults. Lancet. 2018;392:432-46.
33. Eckel-Passow JE, Lachance DH, Molinaro AM, Walsh KM, Decker PA, Sicotte H, et al. Glioma groups based on 1p/19q, IDH, and TERT promoter mutations in tumors. N Engl J Med. 2015;372:2499-508.
34. Tateishi K, Iafrate AJ, Ho Q, Curry WT, Batchelor TT, Flaherty KT, et al. Myc-driven glycolysis is a therapeutic target in glioblastoma. Clin Cancer Res. 2016;22:4452-65.
35. Qian X, Li X, Shi Z, Xia Y, Cai Q, Xu D, et al. PTEN suppresses glycolysis by dephosphorylating and inhibiting autophosphorylated PGK1. Mol Cell. 2019;76:516-27.e7.

36. Wang G, Fu XL, Wang JJ, Guan R, Sun Y, Tony To SS. Inhibition of glycolytic metabolism in glioblastoma cells by Pt3glc combinated with PI3K inhibitor via SIRT3-mediated mitochondrial and PI3K/Akt-MAPK pathway. J Cell Physiol. 2019;234:5888-903.
37. Zhao S, Liu H, Liu Y, Wu J, Wang C, Hou X, et al. miR-143 inhibits glycolysis and depletes stemness of glioblastoma stem-like cells. Cancer Lett. 2013;333:253-60.

Figures

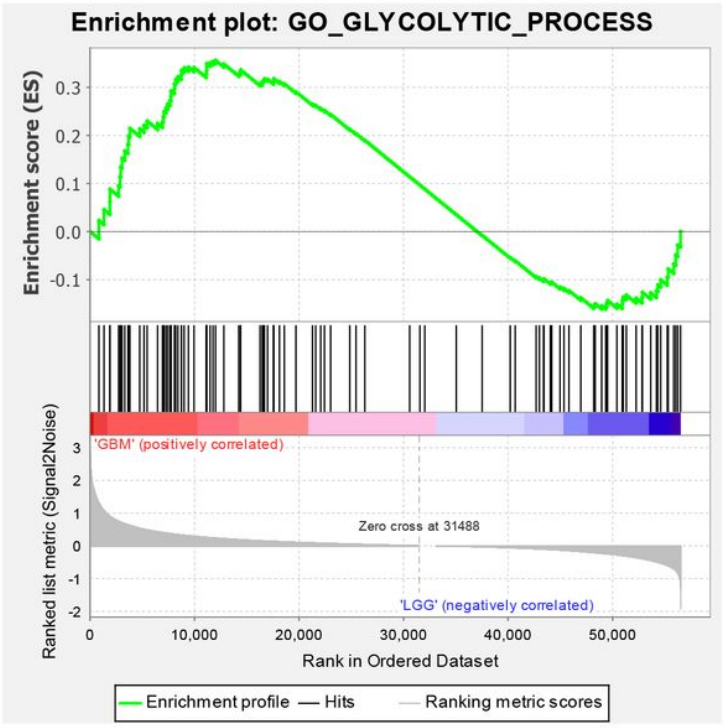

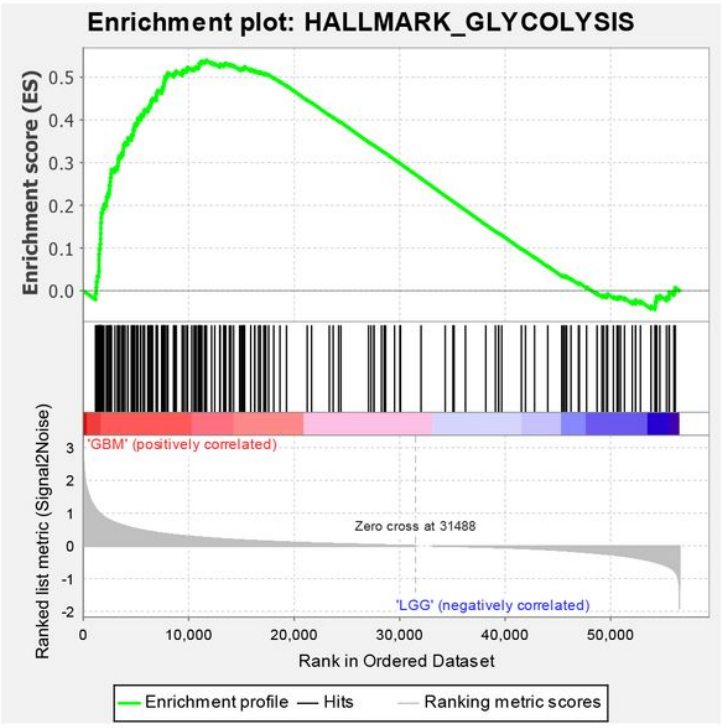

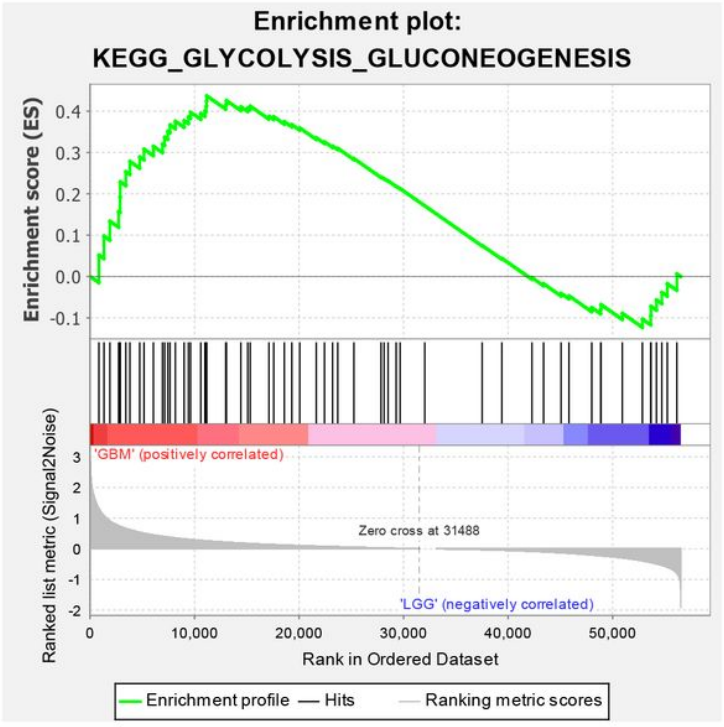

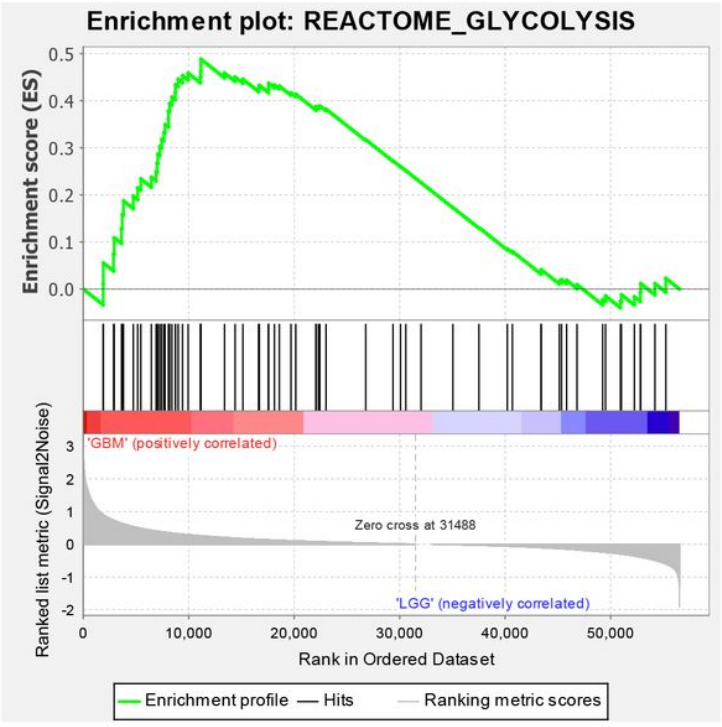

Figure 1

GSEA results of the enrichment plots of four gene sets (GO_GLYCOLYTIC_PROCESS, HALLMARK_GLYCOLYSIS, KEGG_GLYCOLYSIS_GLUCONEOGENESIS, and REACTOME_GLYCOLYSIS) that were significantly differentiated in LGG and GBM samples based on TCGA.

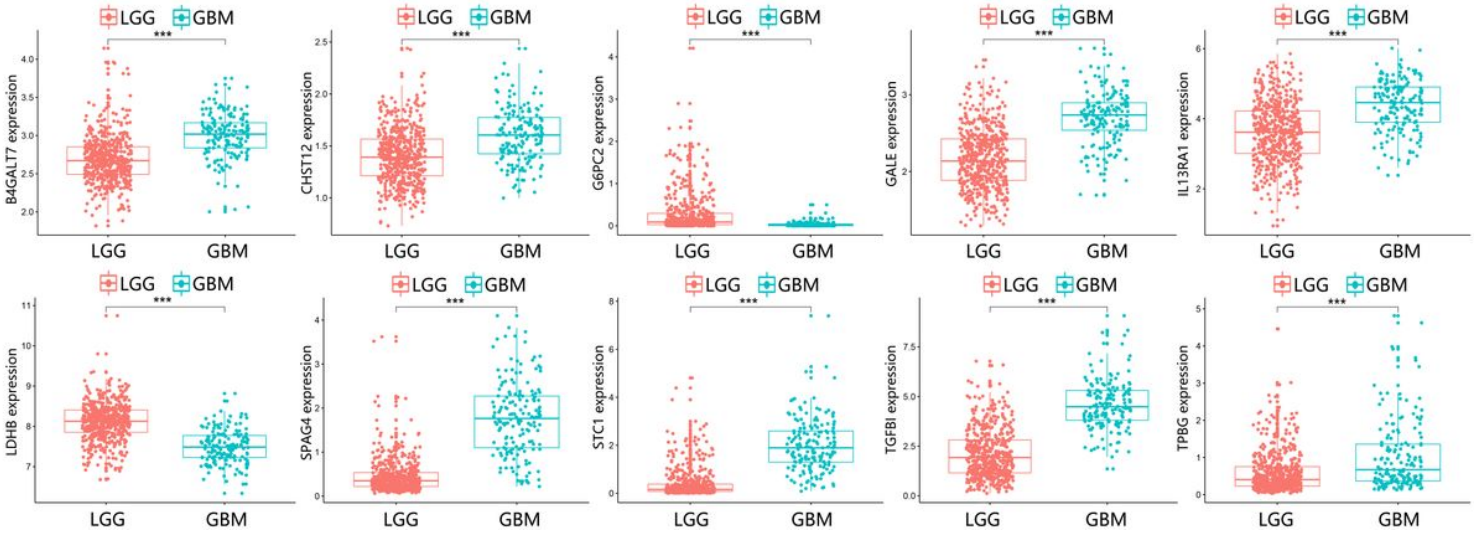

Figure 2

Different expression of ten genes in the LGG (n=529) and GBM (n=168) samples from The Cancer Genome Atlas (***represents p<0.001).

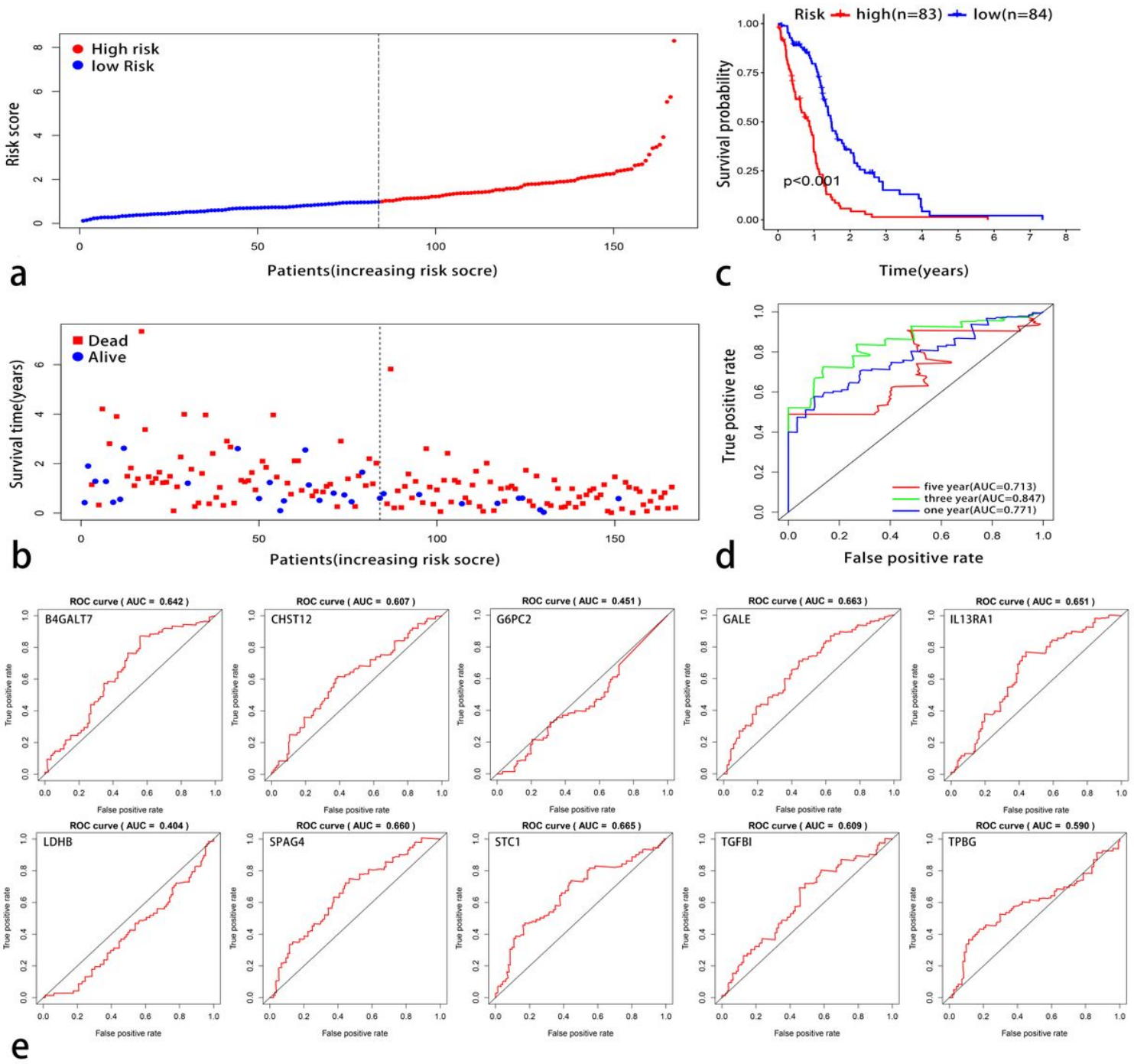

Figure 3

The ten-mRNA signature related to the risk score predicts the overall survival of patients with GBM. (a) Risk score distribution. (b) Survival status. (c) Kaplan-Meier survival curves showed the prognostic value of the risk signature between the low-risk group (n = 84) and the high-risk group (n = 83). (d) ROC curves were used to assess the efficiency of the risk signature for predicting 1-, 3- and 5-year survival. (e) Verifying that the prognostic value of the risk signature is better than that of each single biomarker with ROC curves.

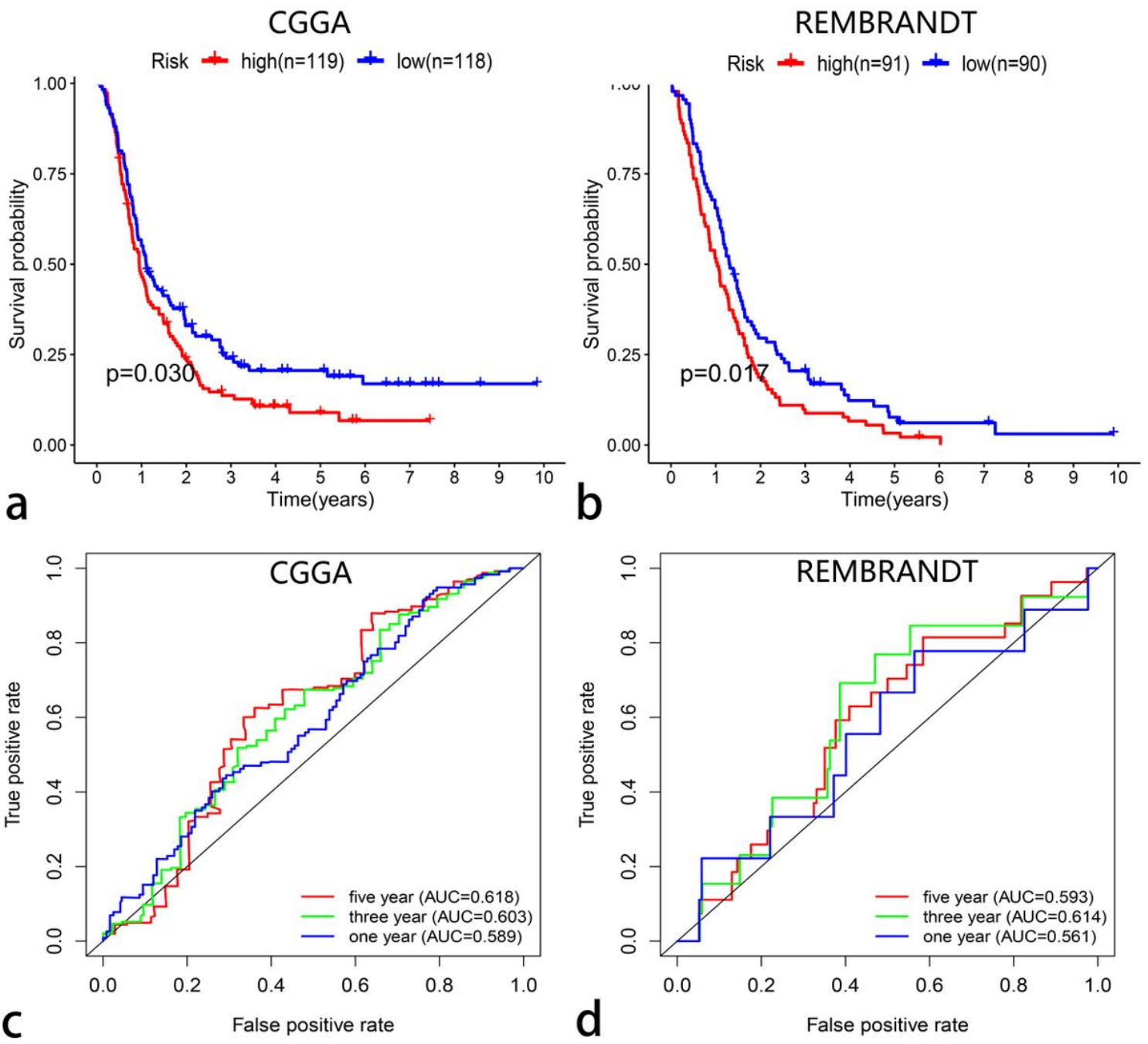

Figure 4

Evaluating the efficiencies of the risk signature in the CGGA and REMBRANDT data sets. a, b, Kaplan-Meier survival curves showed the prognostic value of the risk signature in the CGGA data set (a. low-risk group, n = 118; high-risk group, n = 119; $p<0.05$) and REMBRANDT data set (b. low-risk group, n = 91; high-risk group, n = 90; $p<0.01$). c, d, ROC curves evaluated the efficiency of the risk signature for predicting 1-, 3- and 5-year survival in the CGGA data set (c) and REMBRANDT data set (d).

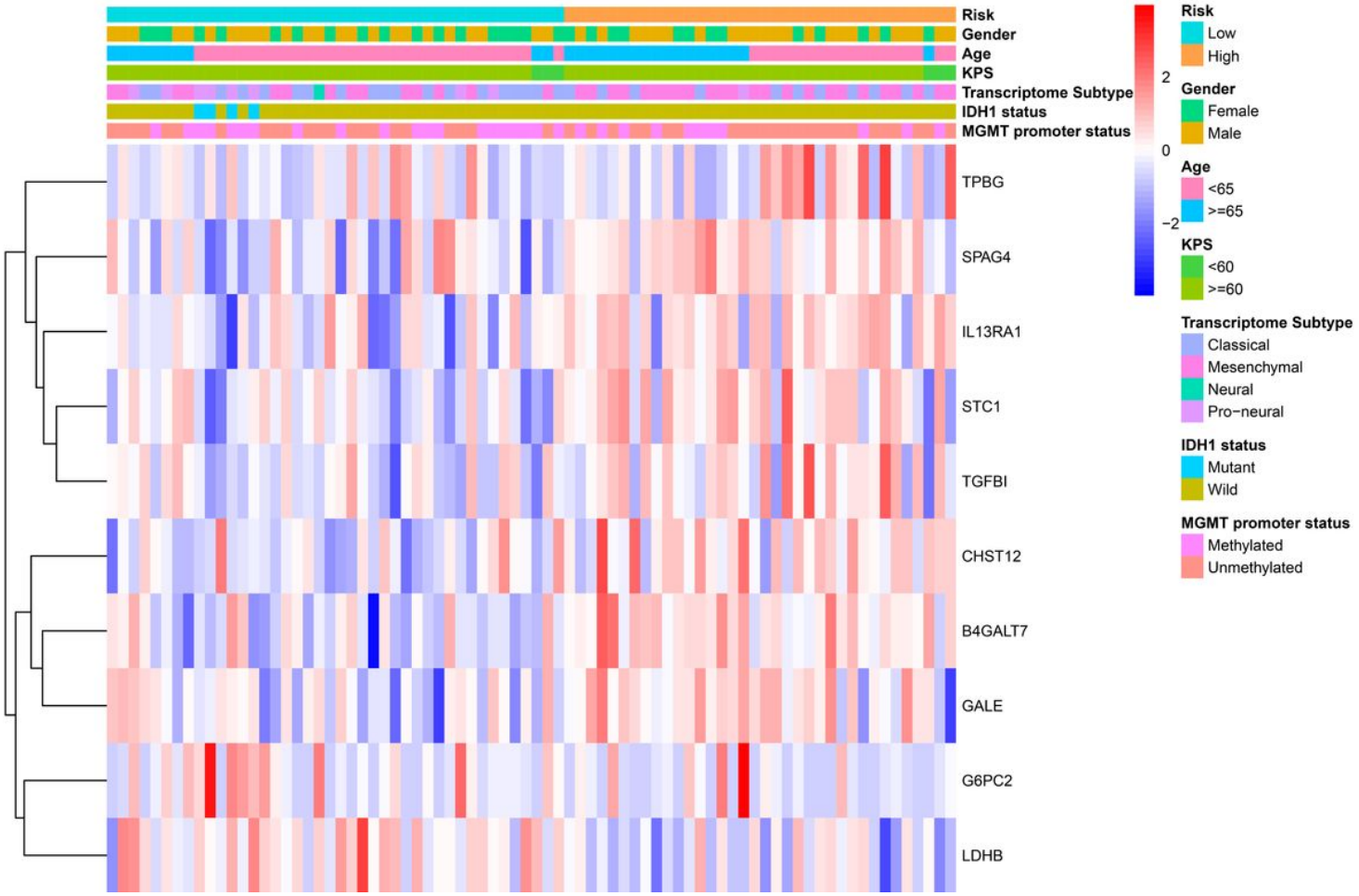

Figure 5

Associations between the signature risk score and clinical features. The heatmap shows the associations between the risk signature and clinical characteristics (gender, age, KPS score, transcriptome subtype, IDH1 status and MGMT promoter status) in the TCGA database.

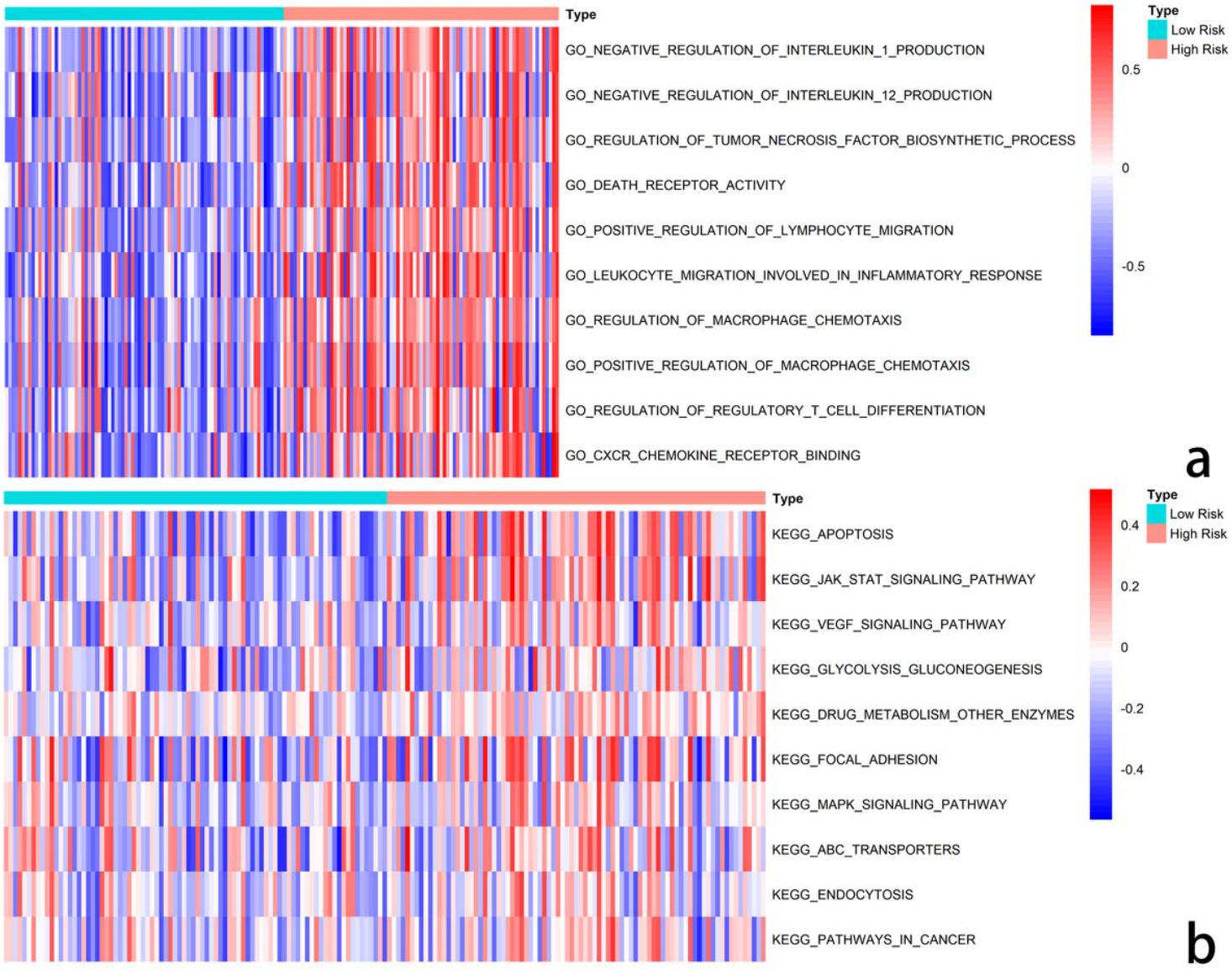

Figure 6

Functional roles of the risk signature. GSVA showed the biological processes (a) and KEGG pathways (b) associated with the risk signature.